Available online at www.sciencedirect.com

ScienceDirect

Mendeleev Commun., 2018, **28**, 559–561

Mendeleev Communications

Microwave-assisted synthesis of magnetite nanoparticles possessing superior magnetic properties

Egor M. Kostyukhin[a,b] and Leonid M. Kustov*[a,b,c]

[a] *N. D. Zelinsky Institute of Organic Chemistry, Russian Academy of Sciences, 119991 Moscow, Russian Federation. Fax: +7 499 135 5328; e-mail: lmkustov@mail.ru*
[b] *National University of Science and Technology 'MISIS', 119049 Moscow, Russian Federation*
[c] *Department of Chemistry, M. V. Lomonosov Moscow State University, 119991 Moscow, Russian Federation*

DOI: 10.1016/j.mencom.2018.09.038

The improved one-step microwave-assisted preparation method for small (5–7 nm) magnetite (Fe_3O_4) nanoparticles possessing saturation magnetization values (97–98 emu g^{-1}) close to that of bulk magnetite using oleic acid as the coating agent has been developed.

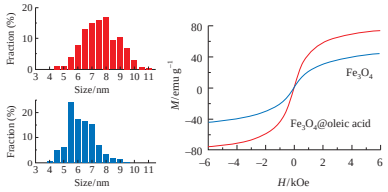

Magnetic nanoparticles with a hydrophobic coating are the promising material for a wide range of applications from drug delivery and solid-state extraction to electronics.[1–6] Their properties directly depend on their size and preparation method.[7–11] Currently, the utilization of magnetic materials with hydrophobic surface is rather limited, however, they are an integral part in the preparation of hydrophilic compounds. This usually includes three steps:[12,13] (i) the synthesis of nanoparticles, (ii) their coating with a hydrophobic compound, and (iii) the consequent preparation of nanoparticles with a hydrophilic surface *via* the ligand-exchange process to replace the hydrophobic groups with hydrophilic ones by the direct coating replacement or functionalization.[14,15] There are many known types of coating agents, including organic compounds, silica, hydroxyapatite, starch, carbon, noble metals, *etc.*,[16–18] while the most widespread ones in the case of nanoparticles are fatty acids,[19,20] especially oleic acid since it is characterized by the strong binding of carboxylic groups to Fe_3O_4 nanoparticles.[21]

However, the deposition of hydrophobic coating onto magnetic magnetite particles has not been adequately described yet, even though it is the important step in the synthesis of such particles. Moreover, a one-step synthesis of hydrophobic nanoparticles coated with oleic acid is also remaining the actual problem, since the application of this acid solution could simplify and accelerate the synthetic process. Attainment of excellent magnetic properties, which depend directly on the size of nanoparticles, their surface properties and crystallinity degree, is also of crucial importance in the development of magnetic materials. The magnetite nanoparticles with a size of about 15–20 nm are well known as possessing the superparamagnetic properties which result in the zero average residual magnetization in the absence of external magnetic field. However, the further decrease of nanoparticle diameter reduces magnetization due to the increased fraction of spin-disordered surface atoms.[22] Taking into account the above problems, this work was aimed at the obtaining of magnetite nanoparticles coated with oleic acid and the estimation of effect of oleic acid amount used on the resulting product, including the investigation of its magnetic properties and size of particles. The obtained samples can be employed in hydrophobic media or be further modified in order to produce materials with hydrophilic surfaces.

According to the previous reports on the preparation of Fe_3O_4 nanoparticles in benzyl alcohol solutions,[23] the optimal time to obtain the small particles in a high yield should not exceed 30 min. The increased time of synthesis leads to the nanoparticles of larger size, while the decreased one results in a low yield and complicated product isolation.[24] Thus, the synthesis of nanoparticles was carried out within 30 min.† The administered concentration of $Fe(acac)_3$ was 31.5 mmol dm^{-3} (see ref. 25). To facilitate steric hindrances and prevent aggregation of magnetic nanoparticles, oleic acid (OA) was selected since the presence of double bond is beneficial for the spatial arrangement of whole carbon chain. However, the increased concentration of oleic acid above 35 mmol dm^{-3} leads also to the difficult isolation of product and formation of 1–2 μm spherical aggregates, which are of no interest in the present work.

X-ray diffraction patterns of prepared Fe_3O_4 samples are shown in Figure 1.‡ The broad peaks observed at 18.29°, 30.08°, 35.42°, 43.05°, 53.41°, and 56.94° for the each sample correspond to the (100), (220), (311), (400), (422) and (333) planes, respectively, according to the diffraction card (JCPDS no. 82-1533). It was shown that the peak intensities decrease along with the increase of oleic acid amount on the nanoparticle surfaces, which indicates the enlarged acid shell. The crystallite size of prepared samples was determined according to the Scherrer equation using the

† The required amounts (0.05 ml, 0.16 mmol; 0.10 ml, 0.32 mmol; 0.2 ml, 0.64 mmol; 0.3 ml, 0.95 mmol; and 0.5 ml, 1.58 mmol) of oleic acid (99%, Sigma-Aldrich) were dissolved in benzyl alcohol (45 ml, 0.43 mol) (99%, Alfa Aesar) under stirring, and Fe^{III} acetylacetonate (0.50 g, 1.42 mmol) (>99%, Acros Organics) was added to the reaction mixture. Once the solution became homogeneous (in about 15 min), it was placed in a Landgraf MW 4000 laboratory microwave oven operating at 2.45 GHz (800 W) for 30 min. The temperature was about 205 °C. The resulting samples were cooled down to room temperature; the nanoparticles were separated by a magnet and washed few times with ethanol. The solid products were dried at 60 °C for 5 h, then collected, and labeled in accordance with the used amount of oleic acid (see Table 1).

‡ XRD patterns were recorded at room temperature for the scanning range (2θ) of 10.0–60.0° at the step of 0.020° and scan speed of 2 deg min^{-1} using a DRON 2 diffractometer equipped with a Cu anode (Kα irradiation, λ = 1.54060 Å).

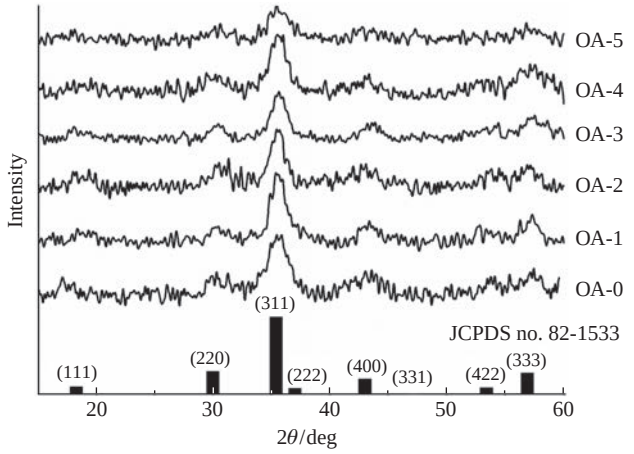

Figure 1 XRD patterns of prepared samples (OA is oleic acid).

full width at the half maximum of peak at 35.6° (Table 1). The smallest average crystallite size was 3.6 nm in the case of sample OA-3. However, the average nanoparticle size is not fully informative due to the growth of XRD determination error at such small size (< 10 nm), which makes the XRD analysis in this case applicable only for the determination of crystal structure in the samples.

Figure 2 shows the size distribution curves plotted on the basis of TEM images[§] (Figure S1, Online Supplementary Materials) of prepared powders. The nanoparticles possessed a spherical shape in the each sample, which indicates the absence of any phase impurities in the form of other iron oxide/hydroxide phases. The particle size distribution exhibits the shape of lognormal distribution function. The acid concentration does not significantly affect the size of particles and its distribution

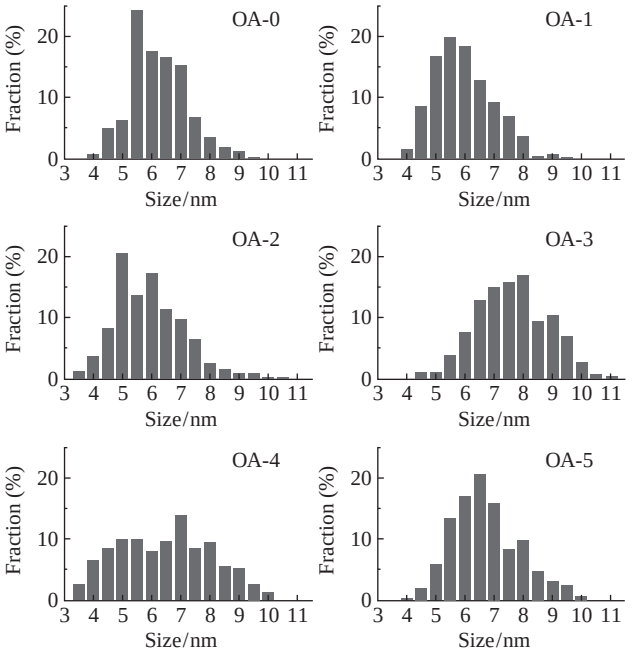

Figure 2 Size distribution curves for the prepared samples.

Table 1 Effect of oleic acid amounts on the size and saturation magnetization of prepared iron oxide nanoparticles.[a]

Sample	Oleic acid/ml	Molar ratio OA/Fe(acac)$_3$[b]	D_{XRD}/ nm	D_{TEM}/ nm	σ/nm	M_S/ emu g^{-1}
OA-0	0	0	5.8	6.4	0.9	56
OA-1	0.05	0.11	7.0	6.1	1.0	66
OA-2	0.10	0.22	3.7	6.0	1.0	68
OA-3	0.20	0.45	3.6	7.9	1.4	97
OA-4	0.30	0.67	5.9	6.8	1.6	98
OA-5	0.50	1.12	5.3	6.5	1.3	84

[a] D_{XRD} is the volume weighted XRD crystallite size; D_{TEM} is the number weighted TEM nanoparticles median diameter; σ is the standard deviation calculated using the D_{TEM} data; and M_S is the saturation magnetization. [b] In the initial solution.

(see Table 1), which may be caused by the formation of complex intermediate in the form of iron oleate, and also by the adsorption of free acid molecules on the surface of formed nanoparticles. At low acid concentrations, the average size of nanoparticles was slightly reduced. An increase in the molar ratio of reagents over 0.22 (OA-2 sample) leads to the growth of nanoparticle sizes and the broadened distribution. The formation of smallest particles was observed at the molar ratio of 0.22 (OA-2 sample), while the smallest value of the standard deviation was achieved in the absence of oleic acid (OA-0 sample). The distribution broadening along with increasing acid concentration probably occurred, since the nanoparticles formation can proceed *via* the two mechanisms: (i) the direct decomposition of iron acetylacetonate to magnetite and (ii) the decomposition of iron acetylacetonate affording an iron oleate intermediate with the consequent magnetite formation, which results in the different nanoparticle sizes. Once nanoparticles have reached a certain critical size, the acid shell acts as the surface stabilizer preventing the further aggregation. Nevertheless, all the prepared samples were characterized by the extremely narrow distribution of particle sizes, which resulted from the uniform heating of mixture volume by the microwave irradiation without any temperature gradient. Thus, the particle growth occurs in the reaction mixture under the similar conditions to produce uniform particles during the short time interval.

The magnetization curves are shown in Figure 3.[¶] There is no coercive field in all cases, while the reversible hysteresis behavior indicates the superparamagnetism for all the prepared samples. The application of oleic acid as the coating agent leads clearly to the increased values of saturation magnetization (M_S) up to 97–98 emu g^{-1} at room temperature in the case of OA-3 and OA-4 samples (see Table 1), which is close to M_S value of bulk

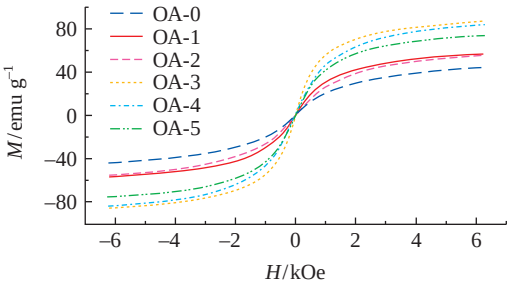

Figure 3 Magnetization curves of prepared Fe_3O_4 samples.

[§] The morphology was investigated using a Hitachi HT7700 transmission electron microscope with resolution of 0.20 nm at 100 kV for the standard pole piece. A target-oriented approach was selected for the optimization of analytic measurements.[32,33] The samples were mounted on a 3 mm copper grid and fixed in a grid holder before the measurements. The images were acquired in the bright-field TEM mode at the accelerating voltage of 100 kV. Core size distributions were estimated on the measurement of at least 200 cores per sample.

[¶] Magnetic measurements were performed using a vibrating magnetometer[34] at ambient temperature (300 K) in the magnetic field of up to 6.3 kOe in both directions. The samples (10–20 mg) were placed between two gas-permeable quartz membranes in a flow-type quartz measuring cell of the magnetometer. Saturation magnetization was calculated by extrapolating the magnetization values *vs.* the inverse of field curve to $H^{-1} = 0$.[35] The measurement accuracy was within 5%.

magnetite (92–100 emu g^{-1}).[26,27] According to some works,[28–30] the oleic acid application as the stabilizer caused the decrease in saturation magnetization of prepared nanocomposites, which, in authors' opinion, was due to the formation of magnetically-dead layer on the nanoparticle surface by oleic acid and to the enlargement of diamagnetic organic phase in the material. However, we have achieved the opposite effect: the one-step synthesis with oleic acid leads to an increase in the saturation magnetization with the maximum at the molar ratio of 0.45–0.67 (OA-3 and OA-4 samples), which can be interpreted in terms of an obviation of canted spins on the disordered surface of nanoparticles.[31] Alternatively, this effect can be explained by the formation on the nanoparticle surface of minor amount of different non-stoichiometric iron oxide phase, but its detection is a crucial task for Mössbauer spectroscopy and to date still being a big challenge.[26] The surface of magnetite nanoparticles can easily be oxidized resulting in the formation of maghemite phase and decreasing the value of saturation magnetization, while the oleic acid as a surfactant in the one-pot process prevents to some extent the interaction between the magnetite surface and oxygen in air, thereby suppressing the undesired phase formation. Nanoparticles prepared *via* a multiple-stage process (including the nanoparticles preparation and their stabilization by the surfactant) can react with air after the first stage, and thus prepared oxidized nanoparticles are covered by an acid. Therefore, the addition of acid in such a manner does not improve magnetization. The saturation magnetization decreases also with further raising the OA/Fe molar ratio. This effect can be associated with the increased thickness of acid shell, which diminishes the mass percent of magnetic particles in the composite. The improved saturation magnetization values are obviously not provided by the particle size changes, since the 4–10 nm nanoparticles without any acid coating also obtained in the benzyl alcohol solution[23,25] did not demonstrate high values of saturation magnetization.

Therefore, the appropriate combination of nanoparticles preparation *via* the microwave-assisted synthesis with the coating processes results in the simplification and acceleration of their preparation, increased saturation magnetization in the size range of 5–7 nm, up to the values typical of bulk magnetite, and also affects the particle sizes, which can be adjusted according to the requirements set by an application. The prepared nanoparticles possess the acidic hydrophobic surface, which prevents their aggregation and makes them soluble in organic solvents. The obtained results are also valuable in practical aspects, since a further surface modification by a hydrophilic compound can allow one to apply these nanoparticles in the biomedical field, *e.g.*, as a contrast agent employing the fast response to applied magnetic fields with negligible remanence and coercivity. In addition, the prepared samples can be used in hyperthermia applications due to the high saturation magnetization values, which leads to large thermal energy dissipation in the tumor cells. The last but not least, large M_S values provide the better control of movement of nanoparticles in the blood directed by the external magnetic field.[22]

The authors are grateful to the Department of Structural Studies at the N. D. Zelinsky Institute of Organic Chemistry of Russian Academy of Sciences for the provided opportunity to use the electron microscopy.

This work was supported by the RF Ministry of Education and Science (project no. RFMEFI61615X0041).

Online Supplementary Materials

Supplementary data associated with this article can be found in the online version at doi: 10.1016/j.mencom.2018.09.038.

References

1 J. Chomoucka, J. Drbohlavova, D. Huska, V. Adam, R. Kizek and J. Hubalek, *Pharmacol. Res*., 2010, **62**, 144.
2 M. Pastor-Belda, P. Viñas, N. Campillo and M. Hernández-Córdoba, *Food Chem*., 2017, **221**, 76.
3 S. Lee, J. Y. Kim, S. Cheon, S. Kim D. Kim and H. Ryu, *RSC Adv*., 2017, **7**, 6988.
4 O. Mokhodoeva, M. Vlk, E. Málková, E. Kukleva, P. Mičolová, K. Štamberg, M. Šlouf, R. Dzhenloda and J. Kozempel, *J. Nanopart. Res*., 2016, **18**, 301.
5 T. N. Pham, N. A. Lengkeek, I. Greguric, B. J. Kim, P. A. Pellegrini, S. A. Bickley, M. R. Tanudji, S. K. Jones, B. S. Hawkett and B. T. Pham, *Int. J. Nanomedicine*, 2017, **12**, 899.
6 R. Madru, P. Kjellman, F. Olsson, K. Wingårdh, C. Ingvar, F. Ståhlberg, J. Olsrub, J. Lätt, S. Fredriksson, L. Knutsson and S.-E. Strand, *J. Nucl. Med*., 2012, **53**, 459.
7 S. Majidi, F. Z. Sehrig, S. M. Farkhani, M. S. Goloujeh and A. Akbarzadeh, *Artif. Cells Nanomed. Biotechnol*., 2016, **44**, 722.
8 V. P. Ananikov, *ACS Catal*., 2015, **5**, 1964.
9 V. P. Ananikov, K. I. Galkin, M. P. Egorov, A. M. Sakharov, S. G. Zlotin, E. A. Redina, V. I. Isaeva, L. M. Kustov, M. L. Gening and N. E. Nifantiev, *Mendeleev Commun*., 2016, **26**, 365.
10 V. P. Ananikov, D. B. Eremin, S. A. Yakukhnov, A. D. Dilman, V. V. Levin, M. P. Egorov, S. S. Karlov, L. M. Kustov, A. L. Tarasov, A. A. Greish, A. A. Shesterkina, A. M. Sakharov, Z. N. Nysenko, A. B. Sheremetev, A. Yu. Stakheev, I. S. Mashkovsky, A. Yu. Sukhorukov, S. L. Ioffe, A. O. Terent'ev, V. A. Vil', Yu. V. Tomilov, R. A. Novikov, S. G. Zlotin, A. S. Kucherenko, N. E. Ustyuzhanina, V. B. Krylov, Yu. E. Tsvetkov, M. L. Gening and N. E. Nifantiev, *Mendeleev Commun*., 2017, **27**, 425.
11 V. M. Shkinev, Yu. A. Zakhodyaeva, R. Kh. Dzhenloda, O. B. Mokhodoeva and A. A. Voshkin, *Mendeleev Commun*., 2017, **27**, 485.
12 S. Munjal and N. Khare, *J. Nanopart. Res*., 2017, **19**, 18.
13 L. Sun, L. Zhan, Y. Shi, L. Chu, G. Ge and Z. He, *Synth. Met*., 2014, **187**, 102.
14 E. D. Smolensky, H.-Y. E. Park, T. S. Berquó and V. C. Pierre, *Contrast Media Mol. Imaging*, 2010, **6**, 189.
15 D. Ling, M. J. Hackett and T. Hyeon, *Nano Today*, 2014, **9**, 457.
16 B. M. Teo, D. J. Young, and X. J. Loh, *Part. Part. Syst. Char*., 2016, **33**, 709.
17 M. Baghbanzadeh, L. Carbone, P. D. Cozzoli and C. O. Kappe, *Angew. Chem. Int. Ed*., 2011, **50**, 11312.
18 S. Mondal, P. Manivasagan, S. Bharathiraja, M. Santha Moorthy, T. Van Nguyen, H. H. Kim, S. Y. Nam, K. D. Lee and J. Oh, *Nanomaterials*, 2017, **7**, 426.
19 S. Bagheri and N. M. Julkapli, *J. Magn. Magn. Mater*., 2016, **416**, 117.
20 T. A. Lastovina, A. P. Budnyk, M. A. Soldatov, Yu. V. Rusalev, A. A. Guda, A. S. Bogdan and A. V. Soldatov, *Mendeleev Commun*., 2017, **27**, 487.
21 L. Zhang, R. He and H.-C. Gu, *Appl. Surf. Sci*., 2006, **253**, 2611.
22 I. M. Obaidat, B. Issa and Y. Haik, *Nanomaterials*, 2015, **5**, 63.
23 C. Sciancalepore, R. Rosa, G. Barrera, P. Tiberto, P. Allia and F. Bondioli, *Mater. Chem. Phys*., 2014, **148**, 117.
24 D. B. Eremin and V. P. Ananikov, *Coord. Chem. Rev*., 2017, **346**, 2.
25 C. Sciancalepore, F. Bondioli, M. Messori, G. Barrera, P. Tiberto and P. Allia, *Polymer*, 2015, **59**, 278.
26 Z. Kozakova, I. Kuritka, N. E. Kazantseva, V. Babayan, M. Pastorek, M. Machovsky, P. Bazant and P. Saha, *Dalton Trans*., 2015, **44**, 21099.
27 S. Zhao and S. Asuha, *Powder Technol*., 2010, **197**, 295.
28 T. Muthukumaran and J. Philip, *J. Alloys Compd*., 2016, **689**, 959.
29 N. C. C. Lobato, Â. de M. Ferreira and M. B. Mansur, *Sep. Purif. Technol*., 2016, **168**, 93.
30 J. Mosafer, K. Abnous, M. Tafaghodi, H. Jafarzadeh and M. Ramezani, *Colloids Surf., A*, 2017, **514**, 146.
31 M. J. Williams, E. Sánchez, E. R. Aluri, F. J. Douglas, D. A. MacLaren, O. M. Collins, E. J. Cussen, J. D. Budge, L. C. Sanders, M. Michaelis, C. M. Smales, J. Cinatl, Jr., S. Lorrio, D. Krueger, R. T. M. de Rosales and S. A. Corr, *RSC Adv*., 2016, **6**, 83520.
32 V. V Kachala, L. L. Khemchyan, A. S. Kashin, N. V Orlov, A. A. Grachev, S. S. Zalesskiy and V. P. Ananikov, *Russ. Chem. Rev*., 2013, **82**, 648.
33 V. I. Bukhtiyarov, V. I. Zaikovskii, A. S. Kashin and V. P. Ananikov, *Russ. Chem. Rev*., 2016, **85**, 1198.
34 P. A. Chernavskii, G. V. Pankina and V. V. Lunin, *Russ. Chem. Rev*., 2011, **80**, 579 (*Usp. Khim*., 2011, **80**, 605).
35 S. Sathish and S. Balakumar, *Mater. Chem. Phys*., 2016, **173**, 364.

Received: 6th March 2018; Com. 18/5499